DOI:10.7598/cst2016.1186
ISSN:2278-3458

Chemical Science Transactions
2016, **5(3)**, 809-819

RESEARCH ARTICLE

Structure and Dielectric Studies of $LiNi_{0.92}Mg_{0.02}(M)_{0.06}O_2$ (M = Co and Zn) Cathode Materials for Lithium-Ion Batteries

N. MURALI[*1], J. M. SAILAJA[1], TEWODROS AREGAI[2] and V. VEERAIAH[2]

[1]Advanced Analytical Laboratory, DST-PURSE Program,
Andhra University, Visakhaptnam, India
[2]Department of Physics, Andhra University, Visakhapatnam, Andhra Pradesh-530003, India
muraliphdau@gmail.com

Received 4 December 2015 / Accepted 18 December 2015

Abstract: At present, the promising cathode materials for lithium ion batteries are layered structure $LiCoO_2$ and $LiNiO_2$. The $LiCoO_2$ ($LiNiO_2$) have some disadvantages due to structural instability at high temperatures. In the present paper, we discuss the effect of Co, Zn and Mg substitution in $LiNiO_2$ for cathode materials on structural and electrical properties. The layered structure $LiNi_{0.92}Mg_{0.02}(M)_{0.06}O_2$ (M = Co and Zn) cathode materials were synthesized by the solid state reaction method at high temperature. The materials were systematically characterized by TG/DTA, XRD, FESEM, FT-IR and electrical impedance spectroscopy (EIS) studies. The synthesized material has configuration temperature is confirmed from thermogravimetry by differential thermal analysis. All the characterizations show that the cathode materials with their Ni compound substituted by Co, Zn and Mg keep a typical α-$NaFeO_2$ layered structure with $R\bar{3}m$ space group. The FESEM reveals that the particle size of the samples is about 2 to 4 μm. The local cation (Li-O) of the materials is understood from Fourier transform infrared spectroscopy (FT-IR) studies. The electrical conductivity is calculated from the synthesized sample Co content it is found to be 9.26×10^{-6} S cm^{-1} at 110 °C temperature is compared to Zn content. The dielectric constant studies are also discussed through impedance spectroscopy.

Keywords: Layered structure, XRD, FESEM, Impedance

Introduction

High specific energy density and long cycle life are simultaneously required for a high performance discharge, charge discharge lithium-ion battery. Therefore, some aspects should be considered in the design of new electrode materials for lithium-ion batteries. In general, structure, chemical stability and the available redox couples of electroactive materials are the primary points[1-4].

The typical cathode material is layered metal oxides with a general formula of $LiMeO_2$ (Me = M (to make it consistent with the lower one) Transition metal elements such as Co, Ni

and Mn), in which the lithium-ion and Me ion occupy the alternate (111) planes of the rock salt structure. The layered structure $LiNiO_2$ is one of the most shown (known) potential cathode materials for lithium-ion batteries due to its high specific capacity, low cost and low toxicity[5-6].

This compound has the advantage of presenting a higher specific capacity for lithium cycling, nevertheless, it is difficult to prepare in the layered structure due to the tendency of lithium and nickel to disorder, leading to a deterioration of their electrochemical performance. Many researches have been undertaken to search for new cathode materials to overcome these shortcomings[7].

To reduce the cost and to improve the cell voltage and specific energy, other transition and non-transition metals which have fixed/variable oxidation states such as Cr, Mn, Fe, Al, Ca, Mg, Zn, Mn, Co, Cu and Rh are used[8-10] in $LiNiO_2$. In these materials many researchers have been prepared by the sol - gel method, combustion method, co-precipitation method and solid-state reaction method. But, the solid-state reaction method easy to synthesis and low cost, and then we used in this work. In this present paper we report that, the compounds $LiNi_{0.92}Mg_{0.02}M_{0.06}O_2$ (M = Co and Zn) were synthesized through the solid state reaction at 850 °C for 20 hours followed by structural characterization and conductivity studies at different temperatures by impedance spectroscopy.

Preparation and experimental techniques

The cathode compositions were synthesized by a solid-state reaction method from stoichiometric amounts of Li_2CO_3 (Merck 99.9%), MgO (Merck 99.9%) and NiO (Merck 99.9%), CoO (Merck 99.9%) and ZnO (Merck 99.9%).

$$0.5Li_2CO_3 + 0.92NiO + 0.02MgO + 0.06CoO \rightarrow LiNi_{0.92}Mg_{0.02}Co_{0.06}O_2 + gas \uparrow$$

$$0.5Li_2CO_3 + 0.92NiO + 0.02MgO + 0.06ZnO \rightarrow LiNi_{0.92}Mg_{0.02}Zn_{0.06}O_2 + gas \uparrow$$

A slight excess amount of lithium (5%) was used to compensate for any loss of the metal which might have occurred during the calcination at high temperatures. The mixture of the starting materials was sufficiently mixed and after grinding the powder it was then heat treated in air at 500 ºC for 5 h and it was again grounded and mixed, and calcined again at 750 ºC for 20 h. Then, this powder was cooled at the rate of 5 ºC/ min. Finally, the powder was ground and mixed and calcined again at 850 ºC for 20 h in air using a muffle box furnace. The powder samples added with polyvinyl alcohol (PVA) as a binder was ground and then pressed at 5 tons / 6 minutes pressure into a circular disk shaped pellet. The pellet was then sintered at 850 °C for 20 h in air at heating and cooling rates of 5° C/min. The surface layers of the sintered pellet were carefully polished and washed with acetone and then the pellet was coated with silver paste on the opposite faces which act as electrodes.

TG/DTA measurements were conducted using Mettler Toledo TG/DTA 851e instrument from room temperature to 1000 °C in a nitrogen atmosphere at a heating rate of 10 °C /min. The powder x-ray diffraction (XRD) data of the sample were collected on a Rigaku Cu-Kα diffractometer with diffraction angles of 20º and 80º in increments of 0.02º. The unit cell lattice parameter was obtained by the least square fitting method from the d-spacing and (hkl) values. Further, the crystal size of the sample was obtained by applying the Scherrer's equation from XRD pattern. The particle morphology of the powders was observed using a field effect scanning electron microscopy image taken from CarlZeiss, EVOMA 15, Oxford Instruments, Inca Penta FETx3.JPG. Fourier transform infrared (FT-IR) spectra were obtained on a Shimadzu FT-IR-8900 spectrometer using a KBr pellet technique in the wave number

range between 350 and 800 cm^{-1}. The impedance study was performed by a Hioki 3532-50 LCR Hitester in the frequency range 42 Hz to 5 MHz at temperature range from room temperature to 110 °C.

Results and Discussion

The thermogravimetric and differential thermal analysis was examined in all the synthesized samples. Thermogravimetric analysis exhibits a gradual and an initial weight loss up to about 730 °C due to the initial evaporation of water (below 200 °C) and a subsequent decomposition of precursors (200-730 °C) from the *in situ* formed meta stable complex as shown in Figure 1 (a) and (b). In other words, the decomposition of carbonates with the evolution of gasses followed by the final decomposition which shows the larger exothermic peak observed at 330 °C in the DTA curve, which results in the formation of $LiNiO_2$ and doped samples. Herein, the compound formation process starts at a temperature as low as 600 °C and the same gets completed around[11] 730 °C. However, the samples of the present study have been heat treated up to 850 °C in order to get phase pure and better crystalline product.

From Figure 2 shows the XRD patterns of the synthesized samples of calcined at 850 °C for 20 h in air atmosphere. Both the samples possess the α-$NaFeO_2$ structure of the rhombohedral system with space group $R\bar{3}m$ and no evidence of any impurities. The $R\bar{3}m$ structure is distorted in the c-axis direction of the hexagonal structure[12]. This is reflected by the split of the (006) and (102) peaks and of the (108) and (110) peaks in the XRD patterns. It is evident that electrochemically reactive $LiNiO_2$ showed a larger integrated intensity ratio of the (003) peak to the (1040 peak (I_{003}/I_{104}) and a clear split of the 108 and 110 peaks in its XRD patterns[13]. The degree of cation mixing, *i.e.* displacement of nickel and lithium ions is low if the value of I_{003}/I_{104} is large and the (108) and (110) peaks are clearly split. The value of $(I_{006}+I_{102})/I_{101}$, called the *R*-factor, are known to decrease as the unit cell volume of $Li_yNi_{2-y}O_2$ decrease. The R-factor increases as y in $Li_yNi_{2-y}O_2$ decreases for y near 1.

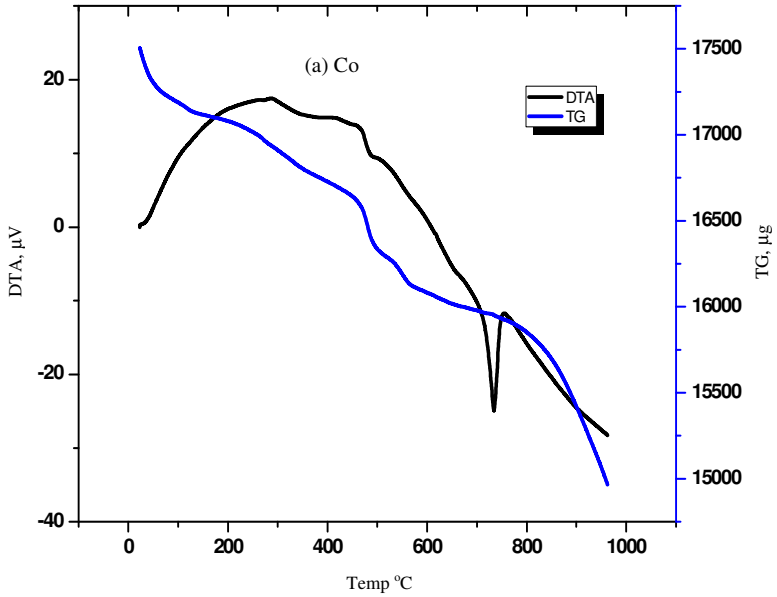

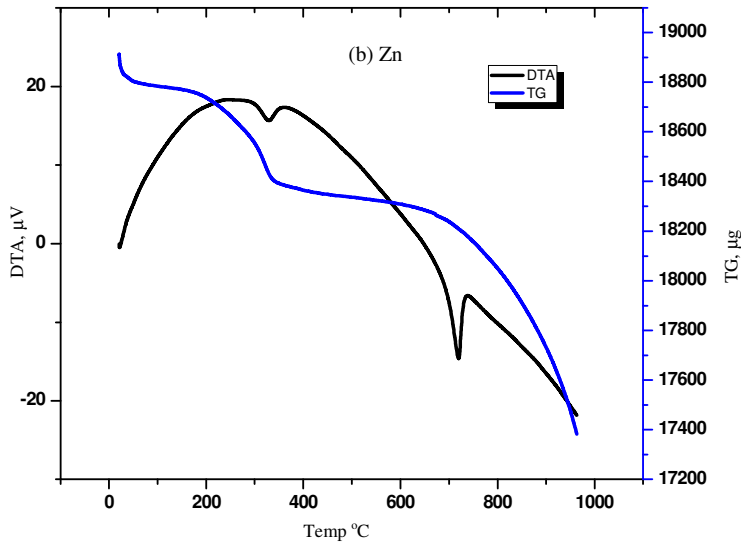

Figure 1. TG/DTA curves for $LiNi_{0.92}Mg_{0.02}(M)_{0.06}O_2$ (M= Co (a) and Zn (b))

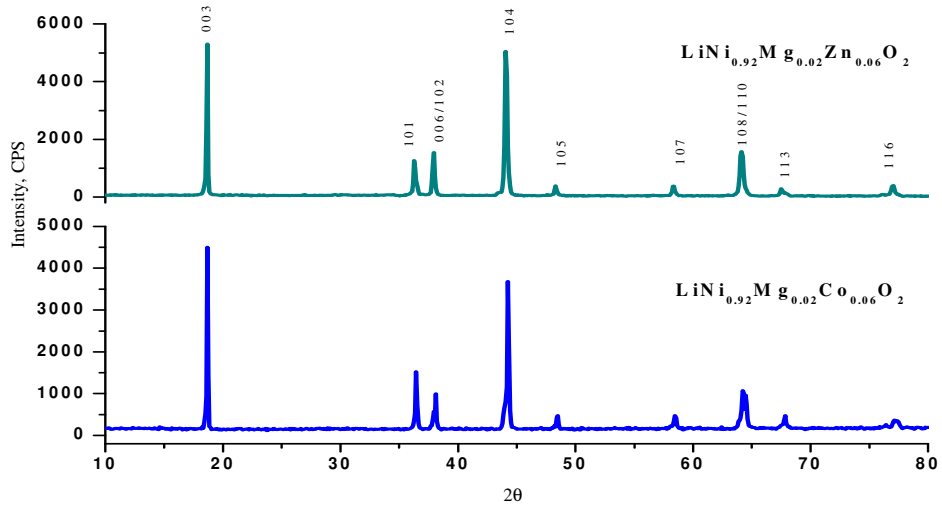

Figure 2. XRD pattern for $LiNi_{0.92}Mg_{0.02}(M)_{0.06}O_2$ (M= Co and Zn)

This indicates that the *R*-factor increases as the degree of cation mixing increases[14-16]. Table 1 presents the values of a, c, c/a, I_{003}/I_{104}, *R*-factor, unit cell volume calculated from XRD patterns of the samples calcined at 850 °C for 20 h in air atmosphere. $LiNi_{0.92}Mg_{0.02}Co_{0.06}O_2$ has the largest value of I_{003}/I_{104} and its value decreases in $LiNi_{0.92}Mg_{0.02}Zn_{0.06}O_2$. But the *R*-factor $LiNi_{0.92}Mg_{0.02}Co_{0.06}O_2$ has the smallest value and its increases in the case of $LiNi_{0.92}Mg_{0.02}Zn_{0.06}O_2$.

The field effect scanning electron microscopy micrographs of $LiNi_{0.92}Mg_{0.02}Co_{0.06}O_2$ and $LiNi_{0.92}Mg_{0.02}Zn_{0.06}O_2$ materials are shown in Figure 3 (a) and (b). It seems that a very fine surface morphology and that the crystal grains[17]. The two samples except that some particles of the $LiNi_{0.92}Mg_{0.02}Zn_{0.06}O_2$ sample are larger than those of the $LiNi_{0.92}Mg_{0.02}Co_{0.06}O_2$.

Table 1. Lattice parameter, unit cell volume, I_{003}/I_{104} and R-factor of $LiNi_{0.92}Mg_{0.02}(M)_{0.06}O_2$ (M= Co and Zn)

Compound	*a* Å	c Å	c/ *a*	Cell volume (Å)3	Crystallite size, nm	Intensity	*R*-factor
$LiNi_{0.92}Mg_{0.02}Co_{0.06}O_2$	2.874	14.24	4.95	101.82	11.02	1.16	0.45
$LiNi_{0.92}Mg_{0.02}Zn_{0.06}O_2$	2.875	14.31	4.98	120.44	8.27	1.05	0.51

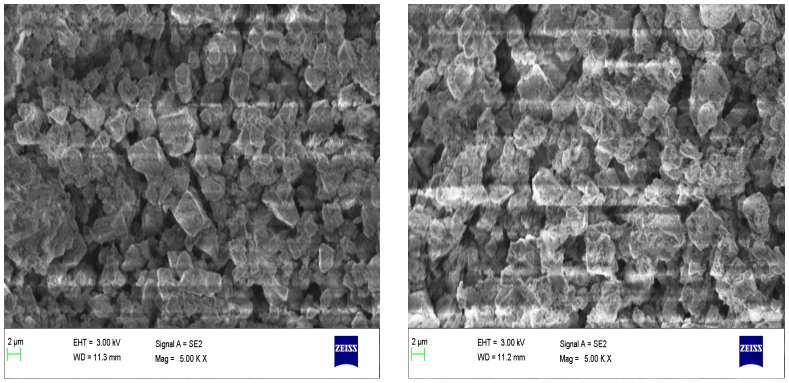

(a) Co (b) Zn

Figure 3. FESEM images for $LiNi_{0.92}Mg_{0.02}(M)_{0.06}O_2$ (M= Co (a) and Zn (b))

Figure 4 (a) and (b) shown the FT-IR spectra of synthesized samples prepared by solid state reaction method calcined at 850 ^oC / 20 h. The band found around 536 cm^{-1}, it has been assigned to Li-O stretching vibration, which indicates the formation of LiO_6 octahedra. The characteristic vibrations of Co-O, Ni-O, Zn-O and Mg-O are 560-590, 579, 611-735 and 630 cm^{-1}, respectively[18]. In this present work, the broadband located at around 638.69 cm^{-1} is attributed to the asymmetric stretching modes of MO_6 (M = Ni, Mg, Co and Zn) group[19]. The wavenumber variation of the synthesized samples for different regions are shown in Table 2.

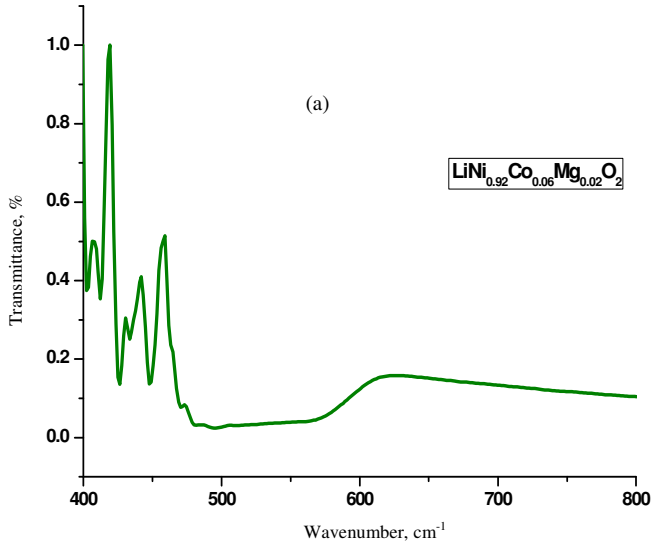

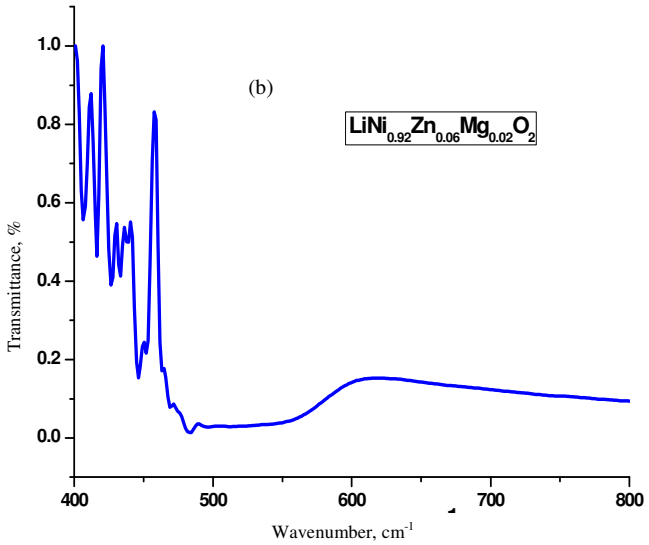

Figure 4. FT-IR spectra for $LiNi_{0.92}Mg_{0.02}(M)_{0.06}O_2$ (M= Co and Zn)

Table 2. FT-IR wavenumber variation of the compounds $LiNi_{0.92}Mg_{0.02}(M)_{0.06}O_2$ (M= Co and Zn)

Compound	Wavenumbers (cm^{-1})			
$LiNi_{0.92}Mg_{0.02}Co_{0.06}O_2$	421.46	476.37	532.13	638.69
$LiNi_{0.92}Mg_{0.02}Zn_{0.06}O_2$	421.53	475.01	533.01	638.69

The electrochemical impedance spectroscopy (EIS) is a powerful technique for understanding electrochemical systems. The conductivity (σ) value has been calculated using the formula,

$$\sigma = \frac{L}{R_b A} S / cm$$

Where, R_b is the bulk resistance of the sample, L is the thickness of the pellet and A is the effective area. The Arrhenius plots of a.c conductivity for $LiNi_{0.92}Mg_{0.02}M_{0.06}O_2$ (M = Co and Zn) are shown in Figures 5 (a) and (b). Curves appear to be close to each other at high temperatures indicting predominance of an onset of intrinsic conductivity mechanism. The conductivity in the cathode materials takes place at low frequencies and it increases with an increase in the temperature is estimated[20]. The calculated a.c conductivity is listed in Table 3.

The activation energy is a phenomenological quantity. It may be said to indicate the free energy barrier an ion has to overcome for a successful jump between the sites. Among the various factors that influence the ionic conductivity of a crystal the activation energy is of utmost importance since the dependence is exponential[21-25]. It can be measured quiet, conveniently by experiments. The activation energies are most commonly deduced using the Arrhenius expression, given by,

$$\sigma = \sigma_0 \exp - \frac{E_a}{k_B T}$$

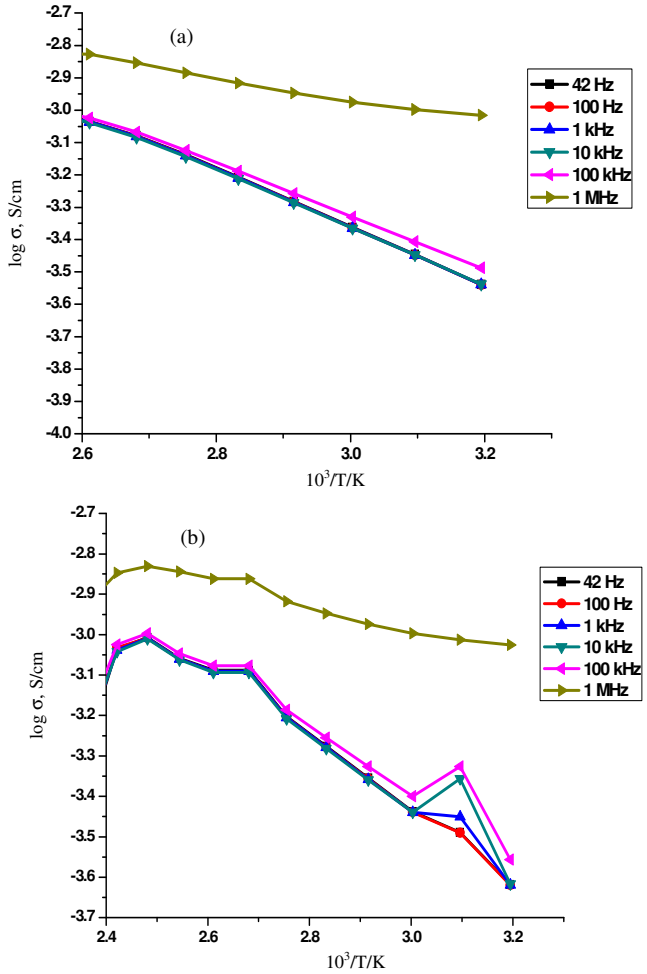

Figure 5. (a) and (b): Arrhenius plots of A.C conductivity for $LiNi_{0.92}Mg_{0.02}(M)_{0.06}O_2$ (M= Co and Zn)

Table 3. ac conductivity values for $LiNi_{0.92}Mg_{0.02}(M)_{0.06}O_2$ (M= Co and Zn)

Temperature °C	AC conductivity, S/cm	
	$LiNi_{0.92}Mg_{0.02}Co_{0.06}O_2$	$LiNi_{0.92}Mg_{0.02}Zn_{0.06}O_2$
30	$3.14x10^{-6}$	$2.01x10^{-6}$
40	$2.89x10^{-6}$	$2.41x10^{-6}$
50	$3.58x10^{-6}$	$3.25x10^{-6}$
60	$4.34x10^{-6}$	$3.65x10^{-6}$
70	$5.23x10^{-6}$	$4.42x10^{-6}$
80	$6.21x10^{-6}$	$5.29x10^{-6}$
90	$7.58x10^{-6}$	$6.27x10^{-6}$
100	$8.34x10^{-6}$	$8.16x10^{-6}$
110	$9.24x10^{-6}$	$8.66x10^{-6}$

Where σ is the conductivity at temperature T in K, k_B is the Boltzmann's constant, E_a is the activation energy and σ_0 is called the pre-exponential factor. The pre-exponential factor, contains all the remaining factors, *i.e.*, other than the activation energy[26-28], that influence the ionic conductivity. The activation energy E_a may be deduced easily from the slope.

The activation energies for $LiNi_{0.92}Mg_{0.02}(M)_{0.06}O_2$ (M = Co and Zn) are in the range of 0.67 to 0.54 eV and 0.19 to 0.75 eV respectively. The calculated activation energies are listed in Table 4. From Figure 6 (a) and (b) show the variation of log σ with frequency for synthesizing samples, it gives the room temperature, conductivity increase, which is attributed to the formation of holes responsible for increased electrical conductivity.

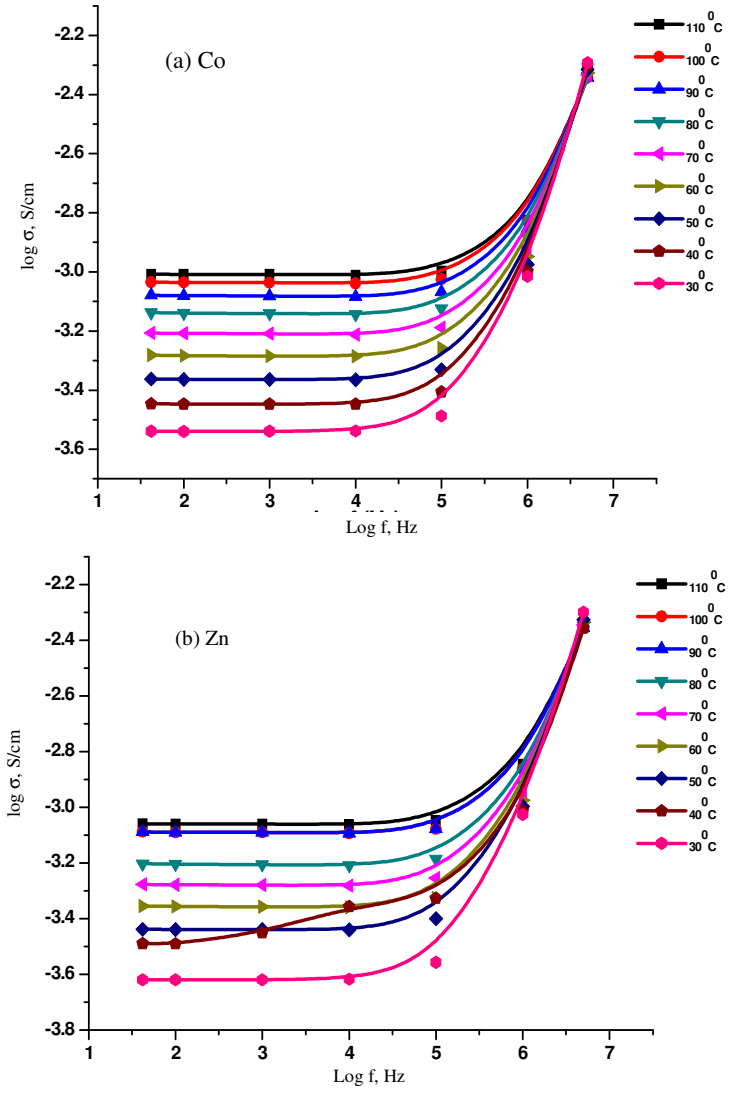

Figure 6. Variation of log σ with frequency for $LiNi_{0.92}Mg_{0.02}(M)_{0.06}O_2$ (M= Co (a) and Zn (b))

Table 4. Activation energy values for $LiNi_{0.92}Mg_{0.02}(M)_{0.06}O_2$ (M= Co and Zn)

Frequency (Hz)	Activation energy (eV)	
	$LiNi_{0.92}Mg_{0.02}Co_{0.06}O_2$	$LiNi_{0.92}Mg_{0.02}Zn_{0.06}O_2$
42	0.29	0.88
100	0.32	0.89
1k	0.43	0.87
10k	0.27	0.81
100k	0.22	0.76
1M	0.26	0.31

Figure 7 (a) and (b) shows the variation of dielectric constant for synthesized samples at from room temperature to 110 ^{0}C. It has been found the dispersion of dielectric constant at the lower frequency range and it maintains constant at higher frequencies[29-31].

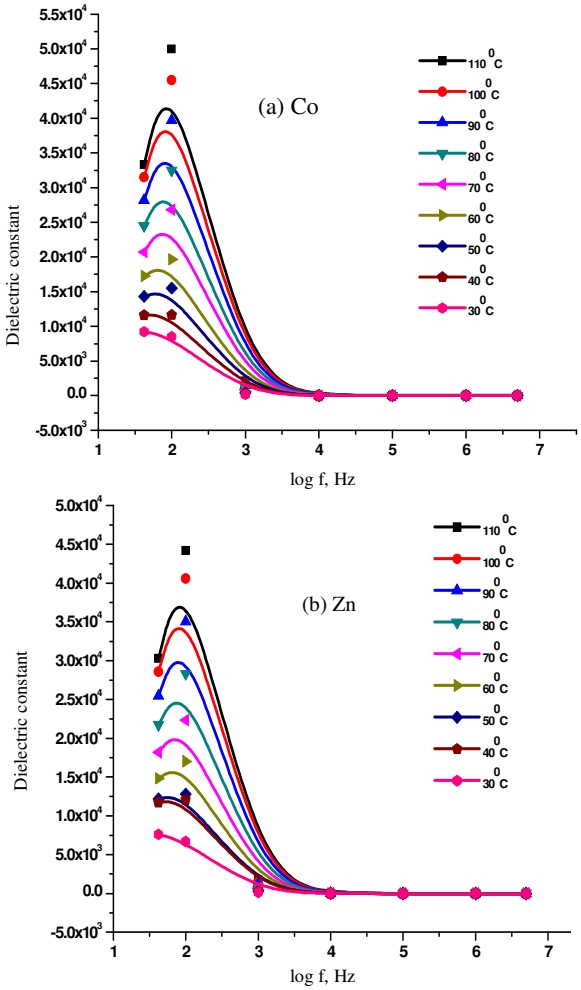

Figure 7. (a) and (b): Frequency dependence of the dielectric constant (εr) of $LiNi_{0.92}Mg_{0.02}(M)_{0.06}O_2$ (M= Co and Zn)

Conclusion

The cathode materials $LiNi_{0.92}Mg_{0.02}(M)_{0.06}O_2$ (M= Co and Zn) are synthesized by the solid state reaction method at high temperature. From x-ray diffraction analysis, both the compounds possess a typical α-$NaFeO_2$ layered structure with $R\bar{3}m$ space group. The FESEM morphology shows a very fine surface morphology and that the crystal grains. The broadband located at around 638.69 cm^{-1} is attributed to the asymmetric stretching modes of MO_6 (M=Ni, Mg, Co and Zn) group from FT-IR spectra. From the impedance measurements $LiNi_{0.92}Mg_{0.02}Co_{0.06}O_2$ found the low conductivity and activation energy. We conclude that the $LiNi_{0.92}Mg_{0.02}Co_{0.06}O_2$ may be suitable for cathode materials due their low activation energy of lithium-ion batteries. The high value of dielectric constant reflects the effect of space charge polarization and/or conducting ionic motion.

References

1. Nagaura T and Tozawa K, *Prog Batt Solar Cells*., 1990, **9,** 209-217.
2. Cho J, Jung H S, Park Y C, Kim G B and Lim H S, *J EIectrochem Soc*., 2000, **147(1)**, 15-20; DOI:10.1149/1.1393137
3. Murali N, Vijaya Babu K, Ephraim Babu K and Veeraiah V, *Mater Sci-Poland*, 2016, **34**(2), 404-411; DOI:10.1515/msp-2016-0038
4. Madhavi S, Subba Rao G V, Chowdari B V R and Li S F Y, *J Power Sources*, 2001, **931-2(),** 156-162; DOI:10.1016/S0378-7753(00)00559-0
5. Murali N, Sailaja J M, Tewodros Aregai, Margarette S J and Veeraiah V, *Int Lett Chem, Phy & Astronomy,*2016, **67**, 31-35; DOI:10.18052/www.scipress.com/ILCPA.67.31
6. Arai H, Okada S, Ohtsuka Y, Ichimura M and Yamaki J, *Solid State Ionics*, 1995, **80,** 261-269; DOI:10.1016/0167-2738(95)00144-U
7. Carl Johan Rydh and Bo Svärd, *Science Total Environment*, 2003, **302(1-3),** 167-184; DOI:10.1016/S0048-9697(02)00293-0
8. Hayner C M, Zhao X and Kung H H, *Annu Rev Chem Biomol Eng*., 2012, **3**, 445-471; DOI:10.1146/annurev-chembioeng-062011-081024
9. Jiang J and Dahn J R, E*lectrochemistry Communications*, 2004, **6(1),** 39-43; DOI:10.1016/j.elecom.2003.10.011
10. Kenji Shizuka, Shouji Takano and Kenji Okahara, *J Power Sources.*, 2007, **174(2)**, 1074-1082; DOI:10.1016/j.jpowsour.2007.06.038
11. Etacheri V, Marom R, Elazari R, Salitra G and Aurbach D, *Energy Environ Sci*., 2011, **4**, 3243-3262; DOI:10.1039/C1EE01598B
12. Seung-Taek Myung, Atsushi Ogata, Ki-Soo Lee, Shinichi Komaba, Yang-Kook Sun and Hitoshi Yashiro, *J Electrochem Soc*., 2008, **155(3),** A374-A383; DOI:10.1149/1.2883733
13. Kalyani P and Kalaiselvi N, *Sci Technology Adv Mater.,* 2005, **6(6),** 689-703; DOI:10.1016/j.stam.2005.06.001
14. Rougier A, Saadouane I, Gravereau P, Willmann P and Delmas C, *Solid State Ionics,* 1996, **90(1-4),** 83-90; DOI:10.1016/S0167-2738(96)00370-0
15. Mizushima K, Jones P C, Wiseman P J and Goodenough J B, *Mater Res Bull*., 1980, **15(6),** 783-789; DOI:10.1016/0025-5408(80)90012-4
16. Mohan Rao M, Liebenow C, Jayalakshmi M, Wulff H, Guth U and Scholz F, *J Solid State Electrochem.*, 2001, **5(5)**, 348-354; DOI:10.1007/s100080000157
17. TONG Dongge, LAI Qiongyu, LU Jizheng, WEI Nini and JI Xiaoyang, *Chinese Science Bulletin*, 2005, **50(11),** 1087-1093; DOI:10.1360/04wb0111

18. Jian Gao, Zhenlei Huang, Jianjun Li, Xiangming He and Changyin Jiang, *Solid State Ionics*, 2014, **20(3-4)**, 301-307; DOI:10.1016/S0167-2738(97)00511-0
19. Chiwei Wang, Xiaoling Ma, Jinguo Cheng, Jutang Sun amd Yunhong Zhou, *J Solid State Electrochem.*, 2007, **11(3)**, 361-364; DOI:10.1007/s10008-006-0150-y
20. Xian-Jun Zhu, Han-Xing Liu, Xiao-Yan Gan, Ming-He Cao, Jian Zhou, Wen Chen, Qing Xu and Shi-Xi Ouyang, *J Electroceram.,* 2006, **17,** 645-649; DOI:10.1007/s10832-006-6705-6
21. Murali N, Vijaya Babu K, Ephraim Babu K and Veeraiah V, *Chem Sci Trans.,* 2014, **3,** 1318-1325; DOI:10.7598/cst2014.850
22. Vijaya Babu K, Veeraiah V, Subba Rao P S V and Paulos S T, *AIP Conference Proceedings*, 2013, **1512**, 1264-1265; DOI:10.1063/1.4791512
23. Myoung Youp Song, Chan Kee Park, Soon Do Yoon, Hye Ryoung Park and Daniel R Mumm, *Electronic Materials Lett.*, 2008, **4(4),** 151-155.
24. Murali N, Vijaya Babu K, Ephraim Babu K and Veeraiah V, *AIP Conference Proceedings*, 2015, **1665**, 140057; DOI:10.1063/1.4918266
25. Nithya C, Syamala Kumari V S and Gopukumar S, *Phys Chem Chem Phys*., 2011, **13,** 6125-6132; DOI:10.1039/C0CP02258F
26. Ping He, Haijun Yu, De Li and Haoshen Zhou, *J Mater Chem*., 2012, **22,** 3680-3695; DOI:10.1039/C2JM14305D
27. Nithya C, Thirunakaran R, Sivashanmugam A and Gopukumar S, *J Power Sources*, 2011, **196(166),** 6788-6793; DOI:10.1016/j.jpowsour.2010.10.053
28. Sambasiva Rao K, Madhava Prasad D and Murali Krishna P, Lee J H, *Physica B,* 2008, **403(12)**, 2079-2087; DOI:10.1016/j.physb.2007.11.031
29. Senthil Kumar P, Sakunthala A, Prabhu M, Reddy M V and Joshi R, *Solid State Ionics,* 2014, **267**, 1-8; DOI:10.1016/j.ssi.2014.09.002
30. Kabi S and Ghosh A, *Eur Phys J B*, 2011, **79,** 377-381; DOI:10.1140/epjb/e2010-10773-8
31. Li Wang, Jiangang Li, Xiangming He, Weihua Pu, Chunrong Wan and Changyin Jiang, *J Solid State Electrochem.*, 2009, **13(8),** 1157-1164; DOI:10.1007/s10008-008-0671-7